

- tissue from differentiated thyroid cancer using Tl-201 and I-131. *J Nucl Med* 1990;31:744.
25. Charke D, Vitti R, Brooks K. Thallium-201 SPECT increases detectability of thyroid cancer metastases. *J Nucl Med* 1990;31:147-158.
 26. Boyd C. Scintigraphic assessment of thyroid cancer. *J Nucl Med* 1990;32:1463.
 27. Ito Y, Muranaka A, Harada T, Matsudo A, Yokobayashi T, Terashima H. Experimental study on tumor affinity of ²⁰¹Tl chloride. *Eur J Nucl Med* 1978;3:81-86.
 28. Nishiyama RH, Dunn EL, Thompson NW. Anaplastic spindle-cell and giant-cell tumors of the thyroid gland. *Cancer* 1972;30:112-127.
 29. Mazzaferri EL, Kemmerer WT, Page CP. Papillary thyroid carcinoma: the impact of therapy in 576 patients. *Medicine* 1977;56:171-196.
 30. Lubin E, Mechlis-Frith S, Zatz S, et al. Serum thyroglobulin and iodine-131 whole-body scan in the diagnosis and assessment of treatment for metastatic differentiated thyroid carcinoma. *J Nucl Med* 1994;35:257-262.
 31. Krishna L, Dadparvar S, Brady LW, et al. Paradoxical changes in iodine-131 scintigraphic findings in advanced follicular thyroid cancer. *J Nucl Med* 1993;34:1574-1576.

Standardized Uptake Value and Quantification of Metabolism for Breast Cancer Imaging with FDG and L-[1-¹¹C]Tyrosine PET

Annemieke C. Kole, Omgo E. Nieweg, Jan Pruijm, Anne M.J. Paans, John Th. M. Plukker, Harald J. Hoekstra, Heimen Schraffordt Koops and Willem Vaalburg

PET Center and Department of Surgical Oncology, Groningen University Hospital, Groningen, The Netherlands; and Department of Surgery, The Netherlands Cancer Institute, Amsterdam, The Netherlands

The aims of the study were to compare the value of L-[1-¹¹C]tyrosine (TYR) and [¹⁸F]fluoro-2-deoxy-D-glucose (FDG) as tumor tracers in patients with breast cancer, to investigate the correlation between quantitative values and standardized uptake values (SUVs) and to estimate the value of SUVs for the evaluation of therapy. **Methods:** Eleven patients with one or more malignant breast lesions and two patients with one or more benign breast tumors were studied with TYR and FDG. Doses of 300 MBq of TYR and 230 MBq of FDG were given intravenously. All PET sessions were performed using a Siemens ECAT 951/31 camera. Of 10 malignant tumors and the 3 benign lesions, glucose consumption and protein synthesis rate were quantified. All lesions were studied using SUVs based on body weight, body surface area and lean body mass, with and without correction for plasma glucose or tyrosine levels. **Results:** All malignant tumors were visualized with both FDG and TYR, but the visual contrast was better with FDG. Increased uptake of the tracers was seen in patients with fibrocystic tissue and complicated the visual assessment and the outlining of tumor tissue. Uptake in fibrocystic disease was more prominent with FDG than with TYR. No difference in tumor/nontumor ratio between the two tracers could be established. FDG showed a false-positive result in one benign lesion. No major differences between the SUVs as defined above were found, although the best correlation between glucose consumption and the SUV was observed when the SUV was based on body surface area and corrected for plasma glucose level ($r = 0.85-0.87$). The SUV based on lean body mass was found to correlate best with protein synthesis rate ($r = 0.83-0.94$). **Conclusion:** In this group of patients, TYR appears to be a better tracer than FDG for breast cancer imaging, because of lower uptake in fibrocystic disease. SUVs correlate well with quantitative values, but future studies must determine whether treatment evaluation is also reliable with SUVs.

Key Words: PET; standardized uptake value; fluorine-18-FDG; carbon-11-tyrosine; breast cancer

J Nucl Med 1997; 38:692-696

Glucose metabolism of many malignant tumors is high compared to normal tissues. This fact is used in PET with the glucose analog [¹⁸F]fluoro-2-deoxy-D-glucose (FDG) to visualize tumors and to analyze and quantify their metabolism. PET

with FDG has proven to be a sensitive method with a high negative predictive value for the visualization of primary breast tumors and the detection of metastases, at least if a correction for attenuation has been made (1-6). However, with FDG, one cannot differentiate between viable tumor tissue and inflammatory tissue, which may cause problems in sequential imaging for treatment evaluation (7,8). Therefore, it would be better to apply tracers such as amino acids that are less avidly metabolized by inflammatory cells. In animal studies, carboxyl-labeled amino acids appeared to be the best amino acids for quantitative PET (9,10). At our institution, L-[1-¹¹C]tyrosine (TYR) is used. Breast cancer can be visualized with this tracer (11,12). The uptake of TYR is increased due to a high protein synthesis rate (PSR) (13), and the PSR can be quantified using the method described by Willemsen et al. (14). Whereas absolute quantification may have its advantages, e.g., in treatment evaluation, quantifying metabolism with PET requires a prolonged study time to calculate a time-activity curve and also requires arterial cannulation or arterialized venous cannulation with repeated blood sampling to obtain the plasma input function. Therefore, a PET study seems to be cumbersome for most patients. In a strive for "unbloody PET," many centers have adopted standardized uptake values (SUVs). This value gives a measure of uptake in the region of interest relative to a uniform distribution over the body. (15) With the application of SUVs, PET is less constraining, due to a shorter acquisition time and the omission of repeat blood sampling. The use of SUVs is widespread, despite reports of considerable drawbacks in their application (16,17). The SUV of many tissues shows a strong positive correlation with weight, because fat has a much lower uptake of both FDG and TYR (Fig. 1). Consequently, results may not be comparable if patients do not have the same weight and habits. When a patient is losing weight during cancer treatment, the PET results using SUVs after therapy should also be interpreted with caution. SUVs based on body surface area (BSA) or lean body mass (LBM) may therefore be preferable to body weight (BW). A quantitative approach would avoid this problem.

In this study, TYR and FDG were compared for their usefulness as a tumor tracer in a group of patients clinically and mammographically suspect for breast cancer. Moreover, the

Received May 9, 1996; revision accepted Sep. 11, 1996.

For correspondence or reprints contact: Annemieke C. Kole, MD, PET Center, Groningen University Hospital, P.O. Box 30.001, 9700 RB Groningen, The Netherlands.

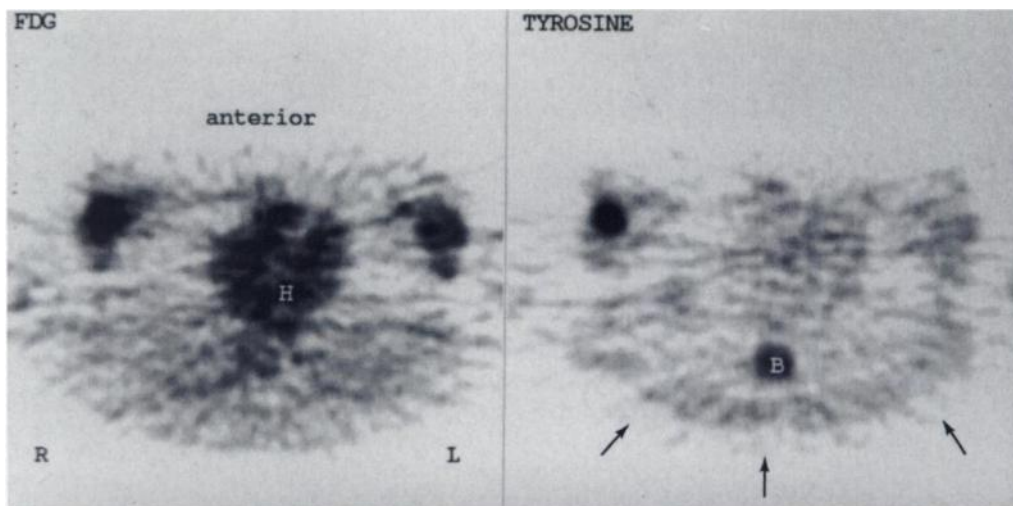


FIGURE 1. Transaxial view of scans with FDG and TYR in a woman with a ductal carcinoma of 4 cm in diameter in the left breast (H = FDG uptake in the heart muscle; B = TYR uptake in the bone marrow). Note the relatively high uptake of FDG in the contralateral breast, and the low uptake of TYR in fat tissue (arrows).

SUV obtained with TYR and with FDG were compared with the quantitative value for PSR and glucose consumption, respectively. SUVs were calculated using BW, BSA and LBM and a correction for plasma tyrosine and glucose levels. The value of SUVs for the evaluation of therapy was estimated.

METHODS

Patients

TYR and FDG were studied in 13 patients with clinically and mammographically malignant breast lesions. The study protocol was approved by the Medical Ethics Committee of the Groningen University Hospital. All patients gave written informed consent. Eleven patients were ultimately proven to indeed have a malignant breast lesion. Two patients had a benign lesion, and in one of these patients two benign lesions were found in the same breast. Histological examination was performed after PET. In three patients with locally advanced breast carcinoma, the diagnosis was confirmed by fine needle aspiration cytology. Patient data are listed in Table 1. All patients fasted overnight before the PET study and had normal plasma glucose (range, 3.1–5.6 mmol/l) and tyrosine levels (range, 35–60 nmol/l).

TYR and FDG Production

TYR was produced via a modified microwave-induced Bücherer-Strecker synthesis (18). The radiochemical purity was over 99%. A mean dose of 300 MBq (range, 55–375 MBq) of TYR was injected intravenously. FDG was routinely produced by a robotic system after the procedure as described by Hamacher et al. (19). The procedures were protocolized to assure a maximum pharmaceutical quality. Radiochemical and chemical purity were verified by high performance liquid chromatography. FDG met the USP XXII requirements and was given in a mean dose of 230 MBq (range, 120–375 MBq) intravenously.

Blood Sampling

All quantitative PET sessions included placement of a catheter in the radial artery for sampling blood radioactivity. During both sessions, blood samples were taken at 0.25, 0.50, 0.75, 1.00, 1.25, 1.50, 1.75, 2.25, 2.75, 3.75, 4.75, 7.50, 12.50, 17.50, 25.00, 35.00 and 45.00 min after injection.

Camera

PET imaging was performed with an ECAT 951/31 camera (Siemens/CTI, Knoxville, TN). A 20-min transmission scan was obtained immediately before the emission scan to correct for photon attenuation by the body tissues. Seven patients underwent a TYR study and an FDG study subsequently, using only one transmission scan for attenuation correction. FDG was injected 80

min after TYR. Both tracers were administered as a 1-min bolus via an infusion pump. These seven patients did not leave the camera between the TYR and FDG studies. The other six patients underwent both studies on successive days, and separate transmission scans were obtained. Dynamic images at the level of the tumor were acquired from the time of injection of the tracer through 50 min after injection: 10 30-sec images, 3 5-min images and 3 10-min images. The same camera protocol was used for both tracers.

Quantitative Analysis

PET images were displayed applying standard ECAT software. To obtain the average metabolic rate of glucose consumption (MRglc), the tumor has to be defined in all relevant planes of the study. In the literature, this is done by placing (multiple) regions of interest (ROIs) in each plane. The tissue time-activity curves obtained from these ROIs is summed and the average MRglc is calculated. As this method is quite laborious, an alternative method was developed as reported previously (12,14). In brief, using the same activity threshold as used for definition of the ROI, all voxels

TABLE 1
Patient Data

Patient no.	Tumor (stage)	Size (cm)	Body weight (kg)	Height (m)
1	Cyst (benign)	5.0	70	1.70
2	Fibroadenoma	1.0	83	1.70
	atypical dysplasia	1.0		
3	Comedo (T1)	2.0	67	1.66
4	Lobular (T1)	1.2	75	1.63
5	Ductal (T2)	2.5	90	1.74
6	Ductal (T2)	3.5	54	1.50
7	Ductal (T2)	3.5	70	1.65
8	Ductal (T2)	4.0	75	1.60
9	Ductal (T2)	4.0	84	1.74
10	Ductal (T2)	4.0	89	1.74
	two metastases			
11	(T4)	4.0	70	1.65
12	(T4)	5.0	90	1.70
13	(T4)	10.0	62	1.59

Size represents maximum tumor diameter, measured at histological examination after resection or mammographically (Patients 1, 11, 12 and 13). The two metastases were not palpable (Patient 10). In Patients 11, 12 and 13, malignancy was confirmed by fine needle aspiration cytology, but no information about histological type is available because these patients did not undergo surgery.

that were above this threshold were selected after masking the study for nontumor tissue with a high activity (e.g., liver and pancreas). The corresponding activity was summed and the average time-activity curve was obtained. The advantage of this approach is that the analysis of the whole tumor is performed quickly and simply, while giving identical results as the ROI method (Willemssen ATM, personal communication). Combining these averaged time-activity data with the plasma glucose level (the plasma input data), the average MRglc (in $\mu\text{mol}/100\text{ ml}$ of tumor tissue/min) was calculated for both tumor and contralateral breast tissue, using the Patlak analysis. Because the lumped constant for FDG in breast and tumor tissue is not known, a lumped constant of 0.42 was assumed (20,21).

To obtain the tumor PSR, the averaged time-activity data were combined with the plasma tyrosine level and the plasma input data, corrected for $^{11}\text{CO}_2$ and ^{11}C proteins. The average PSR (in nmol/ml of tumor tissue/min) was calculated. To allow comparison with the SUV analysis, the maximum MRglc and PSR within the malignant tumors were calculated using the same method, but with a threshold of 95%. The absolute maximum pixel value was not used because the statistical variation of the value of a single pixel would have made the result less reliable.

For each tracer, two ratios were calculated, because different tracers cannot easily be compared due to different metabolisms: the ratio of average uptake in tumor and contralateral tissue, and the ratio of maximum uptake in tumor and contralateral tissue. Technical problems (low injected dose, occlusion of arterial cannula) prevented quantification of metabolism in three patients. In one patient, two axillary metastases were in the field of view. Thus, a total of 13 malignant and 3 benign tumors was studied with both FDG and TYR. Eight primary breast tumors, two occult metastases and three benign lesions were observed in a quantitative manner.

SUV Analysis

The metabolism of all malignant breast tumors was calculated using the SUV analysis. For this calculation, the last two frames of the dynamic study were summed to create the equivalent of one static scan. Thus, the SUVs were calculated from a 20 min scan starting 30 min after injection and were based on BW (SUV_{BW}), BSA (SUV_{BSA}) or on LBM (SUV_{LBM}), using the following empirical equations (22,23):

$$\text{SUV} = \frac{\text{tissue concentration [MBq/g]}}{\text{ID (MBq)/patient BW (g)} V_{\text{BSA}} [\text{m}^2] * 10000 V_{\text{LBM}} (\text{g})}$$

$$\text{LBM} = \text{weight [kg]}$$

$$1.2 * \frac{\text{weight (kg)}}{(\text{height})^2 (\text{cm}^2)} + 0.23 * \text{age (yr)} - 10.8 (\text{if male}) - 5.4$$

$$\text{BSA} = \sqrt{\frac{\text{height (cm)} * \text{weight (kg)}}{3600}}$$

All SUVs were calculated for average tumor activity (avg), maximum tumor activity (max) and contralateral breast tissue (con). For both tracers and all SUV calculation methods, ratios for average uptake in tumor and contralateral tissue and for maximum uptake in tumor and contralateral tissue were calculated. Correction for individual variations in plasma glucose level and plasma tyrosine level was applied by multiplying the SUV with the standardized plasma level, because a high plasma level can induce a low SUV (24,25).

Correlation coefficients between SUVs and quantitative values were calculated with using the two-tailed Pearson. A level of $p \leq 0.01$ was considered to be significant.

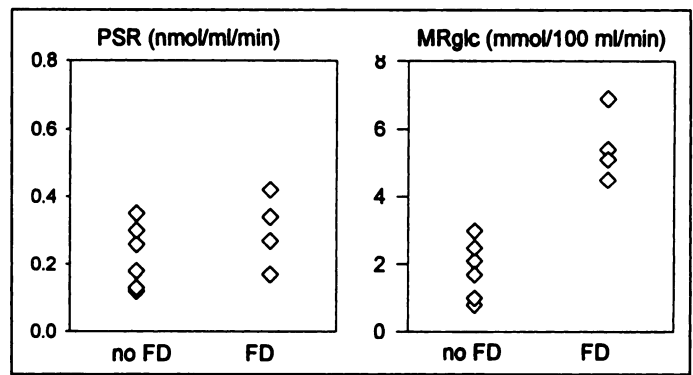


FIGURE 2. PSR and MRglc in the contralateral breast in 10 patients with suspected breast carcinoma who were studied with both tracers quantitatively. FD = fibrocystic disease.

RESULTS

All malignant tumors, including the two metastases, were visualized with both FDG and TYR, although visual contrast was somewhat better with FDG. An example of both radiopharmaceuticals is shown in Figure 1. Of the three benign lesions, the cyst was visualized as a cold spot with both tracers. The other two benign lesions, both in the same patient, were not visualized with TYR. However, a hot spot was seen with FDG. Due to the fact that these lesions were located close to each other ($<0.5\text{ cm}$) in the same breast, it could not be concluded which lesion gave the positive result with FDG.

The mean MRglc was $15.4\ \mu\text{mol}/100\text{ ml}/\text{min}$ (range, 6.4–26.0) with a maximum of 24.3 (7.5–46.3) for the malignant tumors and 3.1 (0.8–6.9) for the contralateral breast. The mean PSR was $1.17\ \text{nmol}/\text{ml}/\text{min}$ (range 0.27–2.92) with a maximum of 1.56 (0.32–3.43) for the malignant tumors and 0.23 (0.07–0.42) for the contralateral breast. Comparison of the two tracers showed similar ratios.

The contralateral breast tissue, which served as control, showed higher uptake in patients with fibrocystic tissue (Fig. 2). Because fibrocystic disease is bilateral, the visual assessment and the outlining of tumor tissue was complicated. The higher uptake of tracer in fibrocystic disease was more prominent with FDG than with TYR.

Mean values and ranges of SUVs are listed in Table 2. SUVs for FDG were generally higher than for TYR. This was observed in tumors and even more pronounced in contralateral breast tissue. SUV ratios tended to be somewhat higher with TYR although no significant difference was reached.

The correlation between quantitative values and SUVs is shown in Table 3. Although differences between the SUV calculation methods were small, for FDG the best correlation

TABLE 2
Average Maximum and Control SUV Based on BW, BSA and LBM in Patients with Malignant Breast Tumors

	FDG	TYR
SUV_{BW} (avg)	3.89 (0.88–7.19)	3.05 (0.92–5.46)
SUV_{BSA} (avg)	0.92 (0.21–1.62)	0.72 (0.22–1.27)
SUV_{LBM} (avg)	2.34 (0.46–4.17)	1.76 (0.40–2.86)
SUV_{BW} (max)	6.32 (2.52–12.24)	5.05 (1.64–10.55)
SUV_{BSA} (max)	1.50 (0.60–2.75)	1.18 (0.39–2.45)
SUV_{LBM} (max)	3.68 (1.31–7.09)	2.88 (0.71–5.39)
SUV_{BW} (con)	0.90 (0.34–2.11)	0.65 (0.20–0.98)
SUV_{BSA} (con)	0.21 (0.08–0.49)	0.16 (0.05–0.25)
SUV_{LBM} (con)	0.55 (0.18–1.36)	0.36 (0.09–0.53)

Mean and range values are shown.

TABLE 3
Correlation Coefficients for Quantitative Values and SUVs

	SUV _{BW}	SUV _{BSA}	SUV _{LBM}	Corrected for plasma glucose and tyrosine		
				SUV _{BW}	SUV _{BSA}	SUV _{LBM}
MRglc (avg)	0.84*	0.87*	0.82*	0.90*	0.91*	0.88*
MRglc (max)	0.83*	0.86*	0.81†	0.90*	0.92*	0.87*
MRglc (con)	0.82†	0.85*	0.77†	0.86*	0.88*	0.84*
PSR (avg)	0.87*	0.89*	0.93*	0.57	0.60	0.65
PSR (max)	0.93*	0.94*	0.94*	0.71	0.74†	0.78†
PSR (con)	0.80†	0.79†	0.83*	0.55	0.58	0.60

*p ≤ 0.001.

†p ≤ 0.01.

was seen with SUVs based on BSA ($r = 0.85-0.87$), and for TYR the best correlation was seen with SUVs based on LBM ($r = 0.83-0.94$). The correlation with FDG increased after correcting the SUV for plasma glucose ($r = 0.87-0.92$), but with TYR, correlation coefficients decreased drastically when the SUV was corrected for plasma tyrosine ($r = 0.71-0.78$). The correlation coefficients for FDG when using SUV_{BSA} corrected for plasma glucose and for TYR using SUV_{LBM} indicate an explained variance (r^2) between 0.77 and 0.85 for FDG and 0.69 and 0.88 for TYR. As a result, 12-31% of the variance of the SUVs is not explained by the correlation.

DISCUSSION

This study demonstrates the potential value of TYR in patients with breast cancer. In this limited group of patients, the visibility of the tumors with TYR was equal to visibility with FDG. TYR uptake was shown to be lower in normal breast tissue (Fig. 2). The use of a SUV analysis appeared to be reliable, although the SUV based on body weight, which is the most frequently used, showed the lowest correlation with the quantitative values.

The vast majority of PET studies with amino acids have been performed with L-[methyl-¹¹C]methionine (MET), which visualizes amino acid transport rather than protein synthesis (26). Kubota et al. (27) investigated the uptake of MET and FDG in a mammary tumor model and found that FDG uptake, in contrast to MET, is enhanced because of tumor-associated macrophages and granulation tissue. In general, an inflammatory reaction is enhanced by chemotherapy and radiotherapy. Therefore, MET may be more suitable for treatment evaluation than FDG (27). Jansson et al. (28) compared the accuracy of MET and FDG in the visualization of primary breast cancers and found that in five out of the seven patients examined with both tracers, MET showed a higher contrast between tumor and surrounding tissue, with the contralateral breast serving as surrounding tissue. Fibrocystic disease is a wastebasket term including a variety of changes such as cysts, stromal fibrosis and proliferative lesions, and is present in at least 50% of women (29). These findings support the hypothesis that, even though FDG uptake in experimental tumors may be higher than MET uptake, other factors in the human breast, of which fibrocystic disease may be an important one, play a disturbing role for FDG. Exact data for TYR are not available, but are expected to show more resemblance to MET than to FDG.

SUVs and quantitative values showed a good correlation for both tracers. No major differences were found between the SUVs calculated by the different methods, although SUV_{LBM} gave the highest correlation coefficients for TYR and SUV_{BSA} for FDG. The widely used SUV_{BW} seemed to be almost equal to the other calculation methods. Schomburg et al. (30) also

found that for FDG the SUV_{BSA} was clearly superior to SUV_{BW} and SUV_{LBM}, while calculating the SUVs in normal lung and liver tissue. However, because normal tissues may show substantial variations over different regions and between patients, comparing the SUVs to the corresponding quantitative values seems absolutely necessary (31). Plasma glucose levels appeared to play a more important role in the correction of the SUV for FDG than plasma tyrosine levels did for TYR. This is in concordance with the findings of Lindholm et al. (24,25) for FDG and MET. High plasma glucose levels may be responsible for lower SUVs, whereas the influence of the plasma amino acid level appears to be more subtle. A linear correction for the plasma tyrosine level implies equal importance of the plasma tyrosine level in TYR calculations and the plasma glucose level in FDG calculations. This is evidently not the case.

The use of SUVs is not without criticism, because there is a variability that cannot be controlled or even has been considered in most reported studies (16,17). Keyes (17) stated the following: "one should standardize the time between tracer administration and data acquisition. Due to recovery coefficients and partial volume effects, the SUV method is not suitable for tumors smaller than 2 cm. The ROI technique should only be used to calculate the maximum pixel value within a ROI." With these restrictions as described for FDG, the SUV can be of value (17). In this study, all but one of these restrictions were encountered: two patients with a tumor smaller than 2 cm in diameter were also studied. One of these patients had two benign lesions, which gave a false-positive signal with FDG. The other patient had a malignant lesion of 1.2 cm in diameter, and both tracers gave a lower signal than was expected. The partial volume effect induced a lower signal in this patient. Instead of calculating the maximum pixel value, which would be unreliable due to statistical variance, we calculated the maximum 5% value.

According to Fischman et al. (32), the major problem using SUVs for FDG studies is that the FDG uptake does not reach a plateau within 90 min after injection and therefore is susceptible to interpretation errors. However, the good correlation coefficients between quantitative values and SUVs for FDG obtained 30 min after injection suggest that this problem is not of practical importance. Anyhow, with TYR this problem is avoided, because TYR uptake reaches its plateau after 20 min.

Yoshida et al. (33) found a good correlation ($r = 0.88$) between quantitative values and SUVs for MET in seven patients. In 22 patients with various type of tumors, a correlation coefficient between SUV_{BW} and PSR of 0.76 was found (12).

PET is well positioned to play an important role in the management of patients with breast cancer. For imaging non-

palpable breast tumors with a higher specificity than conventional mammography, positron emission mammography has recently been introduced (34,35). Considering the high incidence of fibrocystic disease, amino acids such as TYR are more likely to fulfill the specificity expectations.

The use of preoperative chemotherapy for breast cancer is increasingly common. Potentially, PET can predict the outcome of such treatment in an early phase in a noninvasive way. From this study, it was calculated that 69–88% of the variance of SUVs is explained by the correlation with quantitative values. It should be determined in future studies whether this is sufficient to monitor therapy, because the unexplained variance may be larger than the measurable effect of treatment. MET has already been investigated using SUVs for evaluation of chemotherapy in limited groups of patients with breast carcinoma, showing promising results (28,36).

CONCLUSION

In this group of patients, FDG and TYR both visualized breast cancer. An important disadvantage of FDG above the use of TYR is the relatively high uptake in the frequently encountered fibrocystic disease.

High correlations between quantitative values and SUVs were established with both tracers, while no major differences between SUVs based on BW, BSA or LBM were observed. With SUVs, emission scanning time can be shortened and calculations are less technically and mathematically intensive. PET can be performed without assessment of the input function and with reliable results. Future studies are needed to determine whether reliable treatment evaluation is also possible with this noninvasive method.

ACKNOWLEDGMENT

This investigation was financially supported by the Dutch Cancer Society (Koningin Wilhelmina Fonds) Grant RuG 94-786.

REFERENCES

- Wahl RL, Cody R, Hutchins GD, Mudgett EE. Primary and metastatic breast carcinoma: initial clinical evaluation with PET with the radiolabeled glucose analogue 2-[F-18]-fluoro-2-deoxy-D-glucose. *Radiology* 1991;179:765–770.
- Tse NY, Hoh CK, Hawkins RA, et al. The application of positron emission tomographic imaging with fluorodeoxyglucose to the evaluation of breast disease. *Ann Surg* 1992;216:27–34.
- Hoh CK, Hawkins RA, Glaspy JA, et al. Cancer detection with whole-body PET using 2-[18F]fluoro-2-deoxy-D-glucose. *J Comput Assist Tomogr* 1993;17:582–589.
- Nieweg OE, Wong W, Singletary SE, Hortobagyi GN, Kim EE. Positron emission tomography with fluorine-18-deoxyglucose in the detection and staging of breast cancer. *Cancer* 1993;71:3920–3925.
- Adler LP, Crowe JP, Al-Kaisi NA, Sunshine JL. Evaluation of breast masses and axillary lymph nodes with [F-18] 2-deoxy-2-fluoro-D-glucose PET. *Radiology* 1993;187:743–750.
- Bruce DM, Evans NTS, Heys SD, et al. Positron emission tomography: 2-deoxy-2-[18F]-fluoro-D-glucose uptake in locally advanced breast cancers. *Eur J Surg Oncol* 1995;21:280–283.
- Kubota R, Kubota K, Yamada S, Tada M, Ido T, Tamahashi N. Microautoradiographic study for the differentiation of intratumoral macrophages, granulation tissues and cancer cells by the dynamics of fluorine-18-fluorodeoxyglucose uptake. *J Nucl Med* 1994;35:104–112.
- Kubota R, Yamada S, Kubota K, Ishiwata K, Tamahashi T, Ido T. Intratumoral distribution of fluorine-18-fluorodeoxyglucose in vivo: high accumulation in macrophages and granulation tissues studied by microautoradiography. *J Nucl Med* 1992;33:1972–1980.
- Ishiwata K, Kubota K, Murakami M, et al. Re-evaluation of amino acid PET studies: can the protein synthesis rates in brain and tumor tissues be measured in vivo? *J Nucl Med* 1993;34:1936–1943.
- Ishiwata K, Kubota K, Murakami M, Kubota R, Senda M. A comparative study on protein incorporation of L-[methyl-3H]methionine, L-[1-14C]leucine and L-2-[18F]fluorotyrosine in tumor bearing mice. *Nucl Med Biol* 1993;20:895–899.
- Bolster JM, Vaalburg W, Paans AMJ, et al. Carbon-11 labelled tyrosine to study tumor metabolism by positron emission tomography (PET). *Eur J Nucl Med* 1986;12:321–324.
- Kole AC, Pruim J, Nieweg OE, van Ginkel RJ, Hoekstra HJ, Schraffordt Koops H, Vaalburg W. PET with L-[1-11C]-tyrosine for the visualization of tumors and measurement of the protein synthesis rate. *J Nucl Med* 1997;38:191–195.
- Daemen BJ, Elsinga PH, Ishiwata K, Paans AMJ, Vaalburg W. A comparative PET study using different 11C-labelled amino acids in Walker 256 carcinosarcoma-bearing rats. *Int J Radiat Appl Instrum* 1991;18:197–204.
- Willemsen ATM, van Waarde A, Paans AMJ, et al. In vivo protein synthesis rate determination in primary or recurrent brain tumor L-[1-11C]-tyrosine and PET. *J Nucl Med* 1995;36:411–419.
- Zasadny KR, Wahl RL. Standardized uptake values of normal tissues at PET with 2-[fluorine-18]-fluoro-2-deoxy-D-glucose: variations with body weight and a method for correction. *Radiology* 1993;189:847–850.
- Hamberg LM, Hunter GJ, Alpert NM, Choi NC, Babich JW, Fischman AJ. The dose uptake ratio as an index of glucose metabolism: useful parameter or oversimplification? *J Nucl Med* 1994;35:1308–1312.
- Keyes JW. SUV: standard uptake or silly useless value? *J Nucl Med* 1995;36:1836–1839.
- Giron C, Luurtsema G, Vos MG, Elsinga PH, Visser GM, Vaalburg W. Microwave-induced preparation of 11C amino acids via NCA-Bücherer-Strecker synthesis. *J Lab Compd Radiopharm* 1995;37:752–754.
- Hamacher K, Coenen HH, Stocklin G. Efficient stereospecific synthesis of no-carrier-added 18F-fluoro-2-deoxy-D-glucose using aminopolyether supported nucleophilic substitution. *J Nucl Med* 1986;27:235–238.
- Patlak CS, Blasberg RG, Fenstermacher JD. Graphical evaluation of blood-to-brain transfer constants from multiple-time uptake data. *J Cereb Blood Flow Metab* 1983;3:1–7.
- Patlak CS, Blasberg RG. Graphical evaluation of blood-to-brain transfer constants from multiple-time data. Generalizations. *J Cereb Blood Flow Metab* 1985;5:584–590.
- Deurenberg P, Weststrate JA, Seidell JC. Body mass index as a measure of body fatness: age- and sex-specific prediction formulas. *Br J Nutr* 1991;65:105–114.
- Mosteller RD. Simplified calculation of body surface area. *N Engl J Med* 1987;317:1098.
- Lindholm P, Minn H, Leskinen-Kallio S, Bergman J, Ruotsalainen U, Joensuu H. Influence of the blood glucose concentration on FDG uptake in cancer: a PET study. *J Nucl Med* 1993;34:1–6.
- Lindholm P, Leskinen-Kallio S, Kirvela O, et al. Head and neck cancer: effect of food ingestion on uptake of C-11 methionine. *Radiology* 1994;190:863–867.
- Ishiwata K, Vaalburg W, Elsinga PH, Paans AMJ, Woldring MG. Comparison of L-[1-11C]methionine and L-methyl-[11C]methionine for measuring in vivo protein synthesis rates with PET. *J Nucl Med* 1988;29:1419–1427.
- Kubota R, Kubota K, Yamada S, et al. Methionine uptake by tumor tissue: a microautoradiographic comparison with FDG. *J Nucl Med* 1995;36:484–492.
- Jansson T, Westlin JE, Ahlström H, Lilja A, Långström B, Bergh J. Positron emission tomography studies in patients with locally advanced and/or metastatic breast cancer: a method for early therapy evaluation? *J Clin Oncol* 1995;13:1470–1477.
- Love SM, Gelman RS, Silen W. Fibrocystic “disease” of the breast: a nondisease? *N Engl J Med* 1982;307:1010–1014.
- Schomburg A, Bender H, Reichel C, et al. Standardized uptake values of fluorine-18 fluorodeoxyglucose: the value of different normalization procedures. *Eur J Nucl Med* 1996;23:571–574.
- Miyauchi T, Wahl RL. Regional 2-[18F]fluoro-2-deoxy-D-glucose uptake varies in normal lung. *Eur J Nucl Med* 1996;23:517–523.
- Fischman AJ, Alpert NM. FDG-PET in oncology: there's more to it than looking at pictures. *J Nucl Med* 1993;34:6–11.
- Yoshida H, Yoshikawa K, Imazeki K, et al. Correlation analysis between Patlak plot and DAR using 11-C-methionine PET [Abstract]. *Nippon Igaku Hoshasen Gakkai Zasshi* 1995;55:582–586.
- Thompson CJ, Murthy K, Picard Y, Weinberg IN, Mako R. Positron emission mammography (PEM): a promising technique for detecting breast cancer. *IEEE Trans Nucl Sci* 1995;42:1012–1017.
- Weinberg IN, Majewski S, Weisenberger A, et al. Preliminary results for positron emission mammography: real-time functional breast imaging in a conventional mammography gantry. *Eur J Nucl Med* 1996;23:804–806.
- Huovinen R, Leskinen-Kallio S, Nägren K, Lehtikainen P, Ruotsalainen U, Teräs M. Carbon-11-methionine and PET in evaluation of treatment response of breast cancer. *Br J Cancer* 1993;67:787–791.